

Construction of a competitive endogenous RNA network and analysis of potential regulatory axis targets in glioblastoma

Kai Yu

The Second Affiliated Hospital of Nanchang University <https://orcid.org/0000-0003-4145-7464>

Huan Yang

The Second Affiliated Hospital of Nanchang University

Qiao-li Lv

Jiangxi Cancer Hospital

Li-chong Wang

The Second Affiliated Hospital of Nanchang University

Zi-long Tan

The Second Affiliated Hospital of Nanchang University

Zhe Zhang

The Second Affiliated Hospital of Nanchang University

Yu-long Ji

Jiangxi University of Traditional Chinese Medicine

Qian-xia Lin

Jiangxi University of Traditional Chinese Medicine

Jun-jun Chen

Jiangxi Cancer Hospital

Wei He

The Second Affiliated Hospital of Nanchang University

Zhen Chen

The Second Affiliated Hospital of Nanchang University

Xiao-li Shen (✉ shenxldoc@126.com)

<https://orcid.org/0000-0001-9541-3462>

Primary research

Keywords: Glioblastoma, Bioinformatics analysis, Competitive endogenous RNA, differentially expressed genes

Posted Date: September 22nd, 2020

DOI: <https://doi.org/10.21203/rs.3.rs-78209/v1>

License: © ⓘ This work is licensed under a Creative Commons Attribution 4.0 International License. [Read Full License](#)

Version of Record: A version of this preprint was published on February 12th, 2021. See the published version at <https://doi.org/10.1186/s12935-021-01789-z>.

Abstract

Background Glioblastoma is the most common primary malignant brain tumor. Due to the limited understanding of its pathogenesis, the prognosis of glioblastoma is poor. The purpose of this study is to explore potential ceRNA network chains and biomarkers in glioblastoma through integrated bioinformatics analysis. Methods Transcriptome expression data from The Cancer Genome Atlas database and Gene Expression Omnibus were analyzed to identify differentially expressed genes between glioblastoma tissue and normal tissue. The potential biological pathways associated with the differentially expressed genes were explored using Gene Ontology and Kyoto Encyclopedia of Genes and Genomes pathway analysis, and a protein-protein interaction network was established using the STRING database and Cytoscape. Survival analysis using Gene Expression Profiling Interactive Analysis was based on the Kaplan-Meier curve method. The ceRNA network chain was established using the intersection method to align data from four databases (miRTarBase, miRcode, TargetScan, and lncBace2.0), and expression differences and correlations were verified by using quantitative reverse-transcription polymerase chain reaction analysis and determining the Pearson correlation coefficient. Results A total of 2842 DEmRNAs, 2577 DElncRNAs, and 309 DEmiRNAs were dysregulated in glioblastoma. The final ceRNA network consisted of six specific lncRNAs, four miRNAs, and four mRNAs. Among them, four DEmRNAs and one DElncRNA were correlated with overall survival ($p < 0.05$). We found that C1S was significantly correlated with overall survival ($p = 0.015$) and could therefore be used as a biomarker for glioblastoma. Conclusions Four ceRNA networks were established that may influence the occurrence and development of glioblastoma. Among them, the MIR155HG/has-miR-129-5p/C1S axis may be a potential marker and therapeutic target. In particular, C1S has not yet been reported in glioblastoma studies. These findings clarify the role of the ceRNA regulatory network in glioblastoma and lay a foundation for further research.

1. Introduction

Glioblastoma (GBM) is a common malignant primary brain tumor, representing approximately 57 % of all gliomas and 48 % of all primary malignant central nervous system tumors¹. The three standard modes of treatment (maximal surgical resection, radiotherapy, and chemotherapy) result in an average survival of only fourteen months after diagnosis^{2,3}, while without treatment, the life expectancy is less than six months⁴. The limited information on the pathogenesis, development, reproduction, and molecular mechanisms of GBM has hindered the research and development of precise treatments⁵. Therefore, there is an urgent need to clarify the relevant molecular mechanisms of GBM and actively develop new therapeutic strategies.

High throughput sequencing technologies have recently provided oncologists with a powerful tool to identify potential biomarkers for the diagnosis and treatment of cancer. Integrating bioinformatics knowledge with transcriptome sequencing can make data analysis and differential gene identification faster and more accurate^{6,7}. However, there are still some deficiencies in the bioinformatics used to analyze molecular markers and diagnostic indicators of glioma.

A competing endogenous RNA (ceRNA) hypothesis proposed in 2011 described an intricate post-transcriptional regulatory network that mainly includes lncRNAs, microRNAs, mRNAs, circRNAs, and other types of RNAs⁸. Recently, the role of ceRNAs in the process of tumorigenesis and cancer development^{9,10}, including that of lung cancer¹⁰, gallbladder cancer¹⁰, glioblastoma¹¹, gastric cancer¹², pancreatic cancer¹³, and colorectal cancer¹⁴, has been investigated. The ceRNA regulatory network has attracted extensive attention, and many scholars have studied the molecular mechanisms of oncogenesis and development^{15,16}. Nonetheless, few ceRNA networks for GBM have been constructed using bioinformatics analysis.

In our study, to further understand the ceRNA-based regulatory mechanisms in GBM, an aberrant lncRNA-miRNA-mRNA network was constructed using a comprehensive bioinformatics approach. The expression of key RNAs in clinical specimens was analyzed using real-time quantitative reverse-transcription polymerase chain reaction (qRT-PCR). Our study may help researchers gain a comprehensive view of important molecules, identify novel mechanisms underlying glioblastoma pathogenesis, and discover new potential therapeutic targets for the treatment of GBM.

2. Methods

2.1 Microarray data

Three expression profiling datasets [GSE90604 (GPL17692 platform), GSE65626 (GPL17586 platform), and GSE116520 (GPL10558 platform)] and two microRNA expression profiling datasets [GSE65626 (GPL19117 platform) and GSE90604 (GPL21572 platform)] were downloaded from the National Center of Biotechnology Information Gene Expression Omnibus (GEO) (<https://www.ncbi.nlm.nih.gov/geo/>) database. The lncRNA transcriptome data for GBM were downloaded from The Cancer Genome Atlas (<https://cancergenome.nih.gov/>) database. The lncRNA transcription of GBM data included 5 cases of para-cancerous tissues and 156 cases of tumor tissues. The GSE90604 dataset included 16 GBM tissue samples and 7 healthy brain tissue samples, GSE65626 included 6 GBM and 6 healthy brain tissue samples, and GSE116520 included 17 GBM tumor core tissue samples, 17 GBM peritumoral brain zone tissue samples, and 17 healthy brain tissue samples. Two microRNA expression profiling samples were taken from the same datasets, in order to reduce variability between samples. Therefore, we normalized these data using limma software and the edgeR package¹⁷.

2.2 Identification of differentially expressed genes (DEGs)

The four expression profiling datasets used for analysis included CELformat files. These datasets of differential RNA expression in GBM were analyzed in relation to data from normal brain tissue using the limma software package in R. To establish statistical significance, the GSE90604 (miRNA and mRNA) and TCGA datasets were filtered using a cutoff of $(FDR) < 0.01$ and $|Foldchange(FC)| > 1$. GSE65626 (miRNA and mRNA) was filtered using a cutoff of $p < 0.05$ and $|Foldchange(FC)| > 1$. GSE116520 (mRNA) was filtered using a cutoff of $FDR < 0.01$ and $|Foldchange(FC)| > 1.5$. A Venn diagram was constructed using Venny 2.1.

2.3 Gene ontology (GO) and pathway enrichment analysis

GO is widely used in the field of bioinformatics and covers three aspects of biology: biological processes (BP), molecular functions (MF), and cellular components (CC). The Kyoto Encyclopedia of Genes and Genomes (KEGG) is based on the understanding of biological molecular interactions and chemical reactions. We used the Database for Annotation, Visualization, and Integrated Discovery (DAVID) for the analysis of DEGs. Values of $p < 0.05$ and gene counts ≥ 8 were considered statistically significant.

2.4 Protein-protein interaction (PPI) network and gene module analysis

First, the Search Tool for the Retrieval of Interacting Genes (STRING) database was used to obtain DEG-encoded proteins and PPI information. Second, PPI pairs with a combined score > 0.4 were downloaded and analyzed. Then, PPI networks were constructed using Cytoscape software. The plug-in Molecular Complex Detection (MCODE) was used to screen the modules or clusters in large PPI networks. The parameters of DEG clustering and scoring were set as follows: MCODE score > 5 , degree cutoff = 2, node score cutoff = 0.2, max depth = 100, and k-score = 2.

2.5 Survival analysis of DEGs

Gene Expression Profiling Interactive Analysis (GEPIA), a web server for cancer and normal gene expression profiling and interactive analysis, was used to perform survival analysis of the DEGs, confirm their expression, and identify the median expression among tumor and normal samples in BodyMap¹⁸.

2.6 Prediction of target lncRNA-miRNA genes and initial lncRNA-miRNA-mRNA network construction

The initial lncRNA-miRNA-mRNA network was constructed according to the ceRNA hypothesis. miRCODE, the miRTarBase database, and TargetScan were used to predict target DE mRNAs, and only miRNA-mRNAs that were aligned across the three databases were incorporated into the ceRNA network. Next, the DE lncRNA-DE miRNA interactions were predicted, based on the miRCODE database. Cytoscape (Version 3.7.1) was used to construct the preliminary ceRNA network.

2.7 Gene expression and final ceRNA network construction

One-way analysis of variance was used to analyze DEGs and DElncRNAs. The cutoff for the gene expression boxplot was set as $|\text{Log}_2\text{FC}| = 1$ and $p = 0.01$. Then, we used lncBase2.0 and GEPIA (<http://gepia.cancer-pku.cn/index.html>) to validate the DElncRNAs and screen for genes with expression significance, respectively. Finally, we used a Ji mulberry figure to construct the final lncRNA-miRNA-mRNA network.

2.8 RNA isolation and qRT-PCR

Total RNA was extracted from tissues using TRIzol reagent (TaKaRa, Tokyo, Japan) based on the manufacturer's protocol. cDNA was transcribed using the PrimeScript RT Reagent Kit (TaKaRa). The SYBR Green PCR Kit (Takara) was used to detect the quantity of isolated RNA. qRT-PCR was performed using the CFX Connect Real-Time system (Bio-Rad, Hercules, California, USA). PCR amplification was performed as follows: 1 cycle at 95 °C for 5 min, then 50 cycles at 95 °C for 5 s, and finally one cycle at 61 °C for 30 s. GAPDH was used as an internal control. The 2-DDCt method was used to calculate the relative expression levels of the RNAs. The qRT-PCR primers included the bulge-loop RT primer and qPCR primers specific for has-miR-129-5p that were designed and synthesized by RiboBio (Guangzhou, China). *MIR155HG*: F: 5'-CCACCCAATGGAGATGGCTCTA-3', R: 5'-GCAAAAACCCCTATCACGATTA-3'. *C1S*: F: 5'-TCCAAGTCCCATACAACAACTC-3', R: 5'-CAAACCCCGTAAAACGCTCT-3'. *GAPDH*: F: 5'-CCCATCACCCTCTCCAGGAG-3', R: 5'-GTTGTCATGGATGACCTTGGC-3'.

2.9 Statistical analyses

Statistical analyses were conducted using R (version 3.6.1) and SPSS (version 24.0). Differences between groups were determined using a non-parametric *t*-test (the two-sided Wilcoxon test). Correlations among RNA expression were analyzed using Pearson correlation analysis. The chi-square test was used to determine the correlation between expression level and clinicopathological parameters. Values of $p < 0.05$ were considered statistically significant.

3. Results

3.1 Identification of DEGs and differentially expressed mRNAs (DEMs)

In this study, we included 35 patients with GBM and 18 healthy controls. GSE90604, GSE65626, and GSE116520 were analyzed using RStudio software. From the sets of DEGs, a total of 163 genes were identified; among them, 82 were upregulated and the other 81 were downregulated (**Table 1** and **Fig. 2A-D**). Among the DEMs, there were 49 microRNAs identified, including 29 upregulated miRNAs and 20 downregulated miRNAs (**Table 2** and **Fig. 2E**). The top 10 upregulated gene entries were *TM1P1*, *COL4A1*, *TNC*, *CA12*, *PLAU*, *CKS2*, *TMEM45A*, *PLOD2*, *NCAPG*, and *SERPINH1*. The top 10 downregulated gene entries were *CAMK2A*, *OPALIN*, *AK5*, *GRIN1*, *SLC17A7*, *SH3GL3*, *MOBP*, *VSNL1*, *UNC13C*, and *SYN1*.

3.2 Functional and signal pathway enrichment analysis

We uploaded the selected DEGs to the online website DAVID to identify GO terms and KEGG pathways. The DEGs were classified as BP, CC, or MF (**Fig. 3A**). The first two significant functions were selected for analysis (**Fig. 3B**). As shown in Table 3, the results of GO analysis showed that the DEGs were most significantly enriched in the transmission of nerve impulses. Moreover, the upregulated DEGs were significantly enriched in the extracellular matrix (ECM) receptor interaction pathway and basement membrane, and especially in protein binding (**Fig. 3C**). The downregulated DEGs were enriched in functions such as transmission of nerve impulse, synapse, and synapse part (**Fig. 3D**). The results of KEGG pathway analysis indicated enrichment in adrenergic signaling in cardiomyocytes.

3.3 PPI analysis and gene module analysis

A total of 132 DEGs were screened using the STRING online database (<http://string-db.org>) and Cytoscape software. Sixty-seven upregulated genes and 65 downregulated genes were included in the DEG PPI network (**Fig. 4A**), and 30 genes were excluded from the PPI network (132 nodes and 484 edges). After filtering with a cutoff of node degree ≥ 6 criteria, the top 10 hub genes were *SYN1*, *SYT1*, *SNAP25*, *SYN2*, *SLC17A7*, *GRIN1*, *ATP2B2*, *DLG2*, *CAMK2A*, and *SNAP91*. Using Cytoscape's MCODE plug-in, module 1 (score = 9.071), consisting of 29 nodes and 127 edges (**Fig. 4B**), was selected as an important module from the PPI

network. From the functional module genes, the functions of important genes were annotated and analyzed. Functional enrichment analysis showed that module genes were mainly involved in the synaptic vesicle cycle (Fig. 4C).

3.4 Prognostic significance of DEGs

The GEPIA database was used to analyze the GBM overall survival (OS) rate for 20, 40, 60, and 80 months, and the correlation between the DEGs and the survival prognosis of GBM patients was evaluated. The results showed that 12 DEGs (*C1S*, *CFI*, *DCBLD2*, *FAM20C*, *FNDC3B*, *IFI30*, *KDELR2*, *RCAN2*, *PLP2*, *SERPINH1*, *STEAP3*, and *TNFRSF1A*) were significantly correlated with the OS rate in GBM patients ($p < 0.05$) (Fig. 5).

3.5 Construction of ceRNA network

A total of 1,592 DElncRNAs in the TCGA dataset were identified as differential lncRNAs, using the edgeR package (Fig. 6A). miRcode, miRTarbase, and TargetScan were used to predict the miRNA-mRNA pairs (Fig. 6B). Only miRNA-mRNA pairs aligned across the three databases were incorporated into the ceRNA network. Four DEMs fit the requirements of these databases. Then, miRcode was used to predict the potential DEMs targeted by the DElncRNAs (Fig. 6C). According to the ceRNA hypothesis, lncRNA could act as a ceRNA and enhance the expression of target genes through spongy miRNAs. Finally, Cytoscape (Version 3.7.1) was used to verify the initial ceRNA network (Fig. 6D and Table 3).

The first step to further strictly screen the DElncRNAs in the ceRNA network was to screen the highly expressed DElncRNAs from the boxplots in the GEPIA module. The second step was to validate the potential miRNAs targeted by DElncRNAs using the lncBase2.0 database. The third step was to verify the expression of *DLEU2*, *H19*, *HOTAIRM1*, *LINC00152*, *LINC00461*, *MIR155HG*, *C1S*, *DCBLD2*, and *SERPINH1* in GBM tumor tissues and normal brain tissues, using GEPIA and lncBase2.0. Among them, *DLEU2*, *H19*, *HOTAIRM1*, *LINC00152*, *LINC00461*, and *MIR155HG* were identified as DElncRNAs ($p < 0.05$), while *C1S*, *DCBLD2*, and *SERPINH1* were identified as DEmRNAs ($p < 0.05$) (Fig. 7A). The final ceRNA network was then used to construct regulatory axes and included six lncRNAs, four miRNAs, and three mRNAs (Fig. 7B and Table 4).

3.7 Validation of a potential ceRNA axis and correlation analysis of triads

MIR155HG/miR-129-5p/C1S was identified as a potential regulatory axis from the ceRNA network for the following reasons: the results of qRT-PCR analysis indicated that *MIR155HG* (Fig. 8A) and *C1S* (Fig. 8B) were significantly upregulated in GBM ($n = 37$), while *miR-129-5p* (Fig. 8C) was significantly downregulated compared to that in normal brain tissues. Meanwhile, the results of the OS analysis of *MIR155HG* indicated that *MIR155HG* had prognostic value in GBM (Fig. 8D). Then, the glioma RNA sequencing data were downloaded from TCGA and converted into Transcripts Per Million, which was verified by the results of qRT-PCR and the Pearson coefficient correlation. We found that the expression of *MIR155HG /C1S* was positively correlated (Fig. 8E, H), while *miR-129-5p/ MIR155HG* (Fig. 8F, I) and *miR-129-5p/C1S* (Fig. 8G, J) mRNA were negatively correlated. Therefore, *MIR155HG/miR-129-5p/C1S* may be an important potential ceRNA axis.

4. Discussion

Despite the significant progress in comprehensive therapy, the five-year prognosis of glioma patients is still poor^{19,20}. In recent years, there has been great interest in the ceRNA hypothesis. Many studies in this field revolve around how the imbalanced expression of ceRNA affects the pathogenicity and progression of cancer²¹⁻²³. In this study, we used the expression spectrum data of two microRNA and mRNA expression profiling datasets to identify DEGs by means of intersection, ensuring the accuracy of the DEGs. Then, we selected 12 DEGs associated with survival prognosis to construct the ceRNA network and used qRT-PCR to verify a new ceRNA regulatory network that provides new insights into the involvement of ceRNA in the diagnosis and mechanism of glioma, as well as demonstrating the utility of the ceRNA axis as a GBM biomarker.

In this study, a total of 2842 DEmRNAs, 309 DEmiRNAs, and 1592 DElncRNAs were identified. A Venn diagram was used to further reduce and refine these DEGs. By using GO and PPI network analysis, we found that the DEmRNAs were mainly enriched in cell adhesion and ECM-receptor interaction. As examples, the interaction between integrins and ECM promotes chemoresistance by protecting cells from drug-induced apoptosis in several cancer types, including small lung cancer, myeloma,

and ESCC²⁴⁻²⁶. The migration and invasion of glioma cells is a complex combination of multiple molecular processes, including those associated with the ECM, protease secretion, and the actin cytoskeleton, which alter the modification of tumor cell adhesion²⁶.

In general, lncRNAs can act as miRNA sponges, regulating downstream coding genes. miRNAs often adsorb adjacent lncRNAs and mRNAs. First, three databases (miRCODE, miRTarBase, and TargetScan) were used to analyze whether the DEGs and DEMs had binding sites in the gene sequences. Second, the four selected DEMs were used to reverse-predict the potential binding sites of lncRNAs, using two databases (miRCODE and lncBace2.0). Initially, we aimed to build a ceRNA network with 49 DEMs screened from the GEO miRNA microarray datasets. However, when intersected with DElncRNA-DEGs, the DEGs with too many genes and non-critical accounted for the majority. Unexpectedly, among the 163 DEGs, there were 12 related to prognosis and survival. Therefore, we isolated these DEGs and analyzed them separately. Finally, the ceRNA network map was constructed.

The 12 DEGs associated with OS were *C1S*, *CFI*, *DCBLD2*, *FAM20C*, *FNDC3B*, *IFI30*, *KDEL2*, *RCAN2*, *PLP2*, *SERPINH1*, *STEAP3*, and *TNFRSF1A*. Among them, *DCBLD2*²⁷, *FNDC3B*²⁸, *PLP2*²⁹, *SERPINH1*^{30,31}, *STEAP3*^{32,33}, and *TNFRSF1A*³⁴ were abnormally expressed in a series of human tumors. *IFI30* is the most stable prognostic gene of IFN-stimulated genes in glioma³⁵. *CFI* is a potential therapeutic target for nonmelanoma skin cancer³⁶. *C1S*, *FAM20C*, *KDEL2*, and *RCAN2* have rarely been reported in cancer. By building the final ceRNA network chain, we locked the three DEGs of *C1S*, *SERPINH1*, and *SERPINH1*.

The Ji mulberry figure constructed in this study illustrates the four established ceRNA axes: *H19/has-miR-29b-3p/SERPINH1*, *DLEU2/miR-29c-3p/SERPINH1*, *LINC00152 LINC00461/miR-139-5p/DCBLD2*, and *MIR155HG HOTAIRM1 H19/miR-129-5p/C1S*. Phosphorylated *DCBLD2* can recruit *TRAF6* and stimulate the AKT pathway, promoting glioma²⁷. *SERPINH1* expression is related to glioma malignancy and promotes glioma angiogenesis through autocrine and paracrine mechanisms³⁷. *C1S*, as a protease of the classical complement pathway³⁸, has rarely been reported in tumors and has not been studied as an oncogene in gliomas. We identified *C1S* as a new gene that could potentially act as a biomarker in glioma tissue, due to its prognostic and OS predictive value. Additionally, *MIR155HG*, which can also competitively bind *miR-129-5p*, is regarded as an important regulatory factor for hematopoietic, inflammatory, immune, and tumor development processes, as well as other physiological and pathological processes³⁹. *MIR155HG* may be a promising biomarker with the potential to track tumor progression and predict metastasis⁴⁰ and is therefore worthy of further investigation in early patient longitudinal studies.

Although this study established three network relationship chains of ceRNAs and verified a new ceRNA axis, improving our understanding of the role of ceRNA in glioma, there were some limitations. First, verification of the ceRNA axis based only on correlation of differential expression between genes is insufficient, and further verification should be conducted through cell function experiments. Second, three network chains of ceRNAs were identified, but only one ceRNA axis, which has not yet been reported, was selected for verification. To further investigate the mechanism of ceRNA, we have cultured cells for further functional experiments. In conclusion, *C1S* may be a new potential biomarker for GBM. Our findings provide new insights into the role of ceRNA in GBM.

Abbreviations

DElncRNAs: differentially expressed lncRNAs, TCGA: The Cancer Genome Atlas, DEMs: differentially expressed mRNAs, GBM: glioblastoma, qRT-PCR: real-time quantitative reverse-transcription polymerase chain reaction, GEPIA: Gene Expression Profiling Interactive Analysis.

Declarations

Ethics approval and consent to participate

The current study was approved by the Medical Ethics Committee of the Xiangya Hospital of Central South University (No. 201803806). In this study, all procedures were performed in accordance with the Declaration of Helsinki.

Consent for publication

Not applicable.

Availability of data and materials

The datasets used and/or analysed during the current study are available from the corresponding author on reasonable request. The TCGA and GEO datasets could be obtained from online website.

Competing interests

There is no conflicts of interest.

Funding

This study was supported in part by grants from The National Natural Science Foundation of China (81960458, 81860664,81703780), Youth Science Foundation of Science and Technology Department of Jiangxi Provincial(20192BAB215063).

Authors' contributions

SXL planned and supervised the study. YK contributed to conception and design, data acquisition and manuscript drafting. YH, LQL, JYL, LQX, CJJ, TZL, ZZ, HW, CZ collected the glioma tissues and clinical information. All authors drafted the final manuscript. All authors read and approved the final manuscript.

Acknowledgements

Not applicable.

Authors' information

¹Department of Neurosurgery, The Second Affiliated Hospital of Nanchang University, Nanchang, Jiangxi Province, P.R. China.

²Jiangxi Key Laboratory of Translational Cancer Research, Jiangxi Cancer Hospital, Nanchang, Jiangxi, P.R. China. ³Jiangxi University of Traditional Chinese Medicine, Nanchang, Jiangxi, P.R. China.

References

- 1 Ostrom, Q. T. *et al.* CBTRUS Statistical Report: Primary Brain and Other Central Nervous System Tumors Diagnosed in the United States in 2011-2015. *Neuro-Oncology***20**, 1-86, doi:10.1093/neuonc/noy131 (2018).
- 2 Sun, Y., Wang, Z. & Zhou, D. Long non-coding RNAs as potential biomarkers and therapeutic targets for gliomas. *Medical Hypotheses***81**, 319-321, doi:10.1016/j.mehy.2013.04.010 (2013).
- 3 Li, W. & Graeber, M. B. The molecular profile of microglia under the influence of glioma. *Neuro-Oncology***14**, 958-978, doi:10.1093/neuonc/nos116 (2012).
- 4 Lin, T.-K. *et al.* The long non-coding RNA LOC441204 enhances cell growth in human glioma. *Scientific Reports***7**, doi:10.1038/s41598-017-05688-0 (2017).
- 5 Wang, L. *et al.* Screening of differentially expressed genes associated with human glioblastoma and functional analysis using a DNA microarray. *Molecular Medicine Reports***12**, 1991-1996, doi:10.3892/mmr.2015.3659 (2015).
- 6 Kirby, J., Heath, P. R., Shaw, P. J. & Hamdy, F. C. in *Advances in Clinical Chemistry, Vol 44* Vol. 44 *Advances in Clinical Chemistry* (ed G. S. Makowski) 247-292 (2007).
- 7 Vogelstein, B. *et al.* Cancer Genome Landscapes. *Science***339**, 1546-1558, doi:10.1126/science.1235122 (2013).

- 8 Dhamija, S. & Menon, M. B. Non-coding transcript variants of protein-coding genes - what are they good for? *Rna Biology***15**, 1025-1031, doi:10.1080/15476286.2018.1511675 (2018).
- 9 Salmena, L., Poliseno, L., Tay, Y., Kats, L. & Pandolfi, P. P. A ceRNA Hypothesis: The Rosetta Stone of a Hidden RNA Language? *Cell***146**, 353-358, doi:10.1016/j.cell.2011.07.014 (2011).
- 10 Rapicavoli, N. A. *et al.* A mammalian pseudogene lncRNA at the interface of inflammation and anti-inflammatory therapeutics. *Elife***2**, doi:10.7554/eLife.00762 (2013).
- 11 Chiu, Y.-C., Hsiao, T.-H., Chen, Y. & Chuang, E. Y. Parameter optimization for constructing competing endogenous RNA regulatory network in glioblastoma multiforme and other cancers. *Bmc Genomics***16**, doi:10.1186/1471-2164-16-s4-s1 (2015).
- 12 Wu, Q. *et al.* Long non-coding RNA CASC15 regulates gastric cancer cell proliferation, migration and epithelial mesenchymal transition by targeting CDKN1A and ZEB1. *Molecular Oncology***12**, 799-813, doi:10.1002/1878-0261.12187 (2018).
- 13 Yao, K., Wang, Q., Jia, J. & Zhao, H. A competing endogenous RNA network identifies novel mRNA, miRNA and lncRNA markers for the prognosis of diabetic pancreatic cancer. *Tumor Biology***39**, doi:10.1177/1010428317707882 (2017).
- 14 Shan, Y. *et al.* LncRNA SNHG7 sponges miR-216b to promote proliferation and liver metastasis of colorectal cancer through upregulating GALNT1. *Cell Death & Disease***9**, doi:10.1038/s41419-018-0759-7 (2018).
- 15 Sanchez-Mejias, A. & Tay, Y. Competing endogenous RNA networks: tying the essential knots for cancer biology and therapeutics. *Journal of Hematology & Oncology***8**, doi:10.1186/s13045-015-0129-1 (2015).
- 16 Qi, X. *et al.* ceRNA in cancer: possible functions and clinical implications. *Journal of Medical Genetics***52**, 710-718, doi:10.1136/jmedgenet-2015-103334 (2015).
- 17 Ritchie, M. E. *et al.* limma powers differential expression analyses for RNA-sequencing and microarray studies. *Nucleic Acids Research***43**, doi:10.1093/nar/gkv007 (2015).
- 18 Tang, Z. *et al.* GEPIA: a web server for cancer and normal gene expression profiling and interactive analyses. *Nucleic Acids Research***45**, W98-W102, doi:10.1093/nar/gkx247 (2017).
- 19 Lopes, M. B. S. The 2017 World Health Organization classification of tumors of the pituitary gland: a summary. *Acta Neuropathologica***134**, 521-535, doi:10.1007/s00401-017-1769-8 (2017).
- 20 Lapointe, S., Perry, A. & Butowski, N. A. Primary brain tumours in adults. *Lancet***392**, 432-446, doi:10.1016/s0140-6736(18)30990-5 (2018).
- 21 Poliseno, L. *et al.* A coding-independent function of gene and pseudogene mRNAs regulates tumour biology. *Nature***465**, 1033-1039, doi:10.1038/nature09144 (2010).
- 22 Karreth, F. A. *et al.* In Vivo Identification of Tumor-Suppressive PTEN ceRNAs in an Oncogenic BRAF-Induced Mouse Model of Melanoma. *Cell***147**, 382-395, doi:10.1016/j.cell.2011.09.032 (2011).
- 23 Poliseno, L. & Pandolfi, P. P. PTEN ceRNA networks in human cancer. *Methods***77-78**, 41-50, doi:10.1016/j.ymeth.2015.01.013 (2015).
- 24 Xu, Z. *et al.* Integrin beta 1 is a critical effector in promoting metastasis and chemo-resistance of esophageal squamous cell carcinoma. *American Journal of Cancer Research***7**, 531-542 (2017).
- 25 Sethi, T. *et al.* Extracellular matrix proteins protect small cell lung cancer cells against apoptosis: A mechanism for small cell lung cancer growth and drug resistance in vivo. *Nature Medicine***5**, 662-668, doi:10.1038/9511 (1999).

- 26 Damiano, J. S., Cress, A. E., Hazlehurst, L. A., Shtil, A. A. & Dalton, W. S. Cell adhesion mediated drug resistance (CAM-DR): Role of integrins and resistance to apoptosis in human myeloma cell lines. *Blood***93**, 1658-1667, doi:10.1182/blood.V93.5.1658 (1999).
- 27 Feng, H. *et al.* EGFR phosphorylation of DCBLD2 recruits TRAF6 and stimulates AKT-promoted tumorigenesis. *Journal of Clinical Investigation***124**, 3741-3756, doi:10.1172/jci73093 (2014).
- 28 Zhong, Z. *et al.* FNDC3B promotes epithelial-mesenchymal transition in tongue squamous cell carcinoma cells in a hypoxic microenvironment. *Oncology Reports***39**, 1853-1859, doi:10.3892/or.2018.6231 (2018).
- 29 Zimmerman, J. W. *et al.* Cancer cell proliferation is inhibited by specific modulation frequencies. *British Journal of Cancer***106**, 307-313, doi:10.1038/bjc.2011.523 (2012).
- 30 Yamamoto, N. *et al.* Tumor-suppressive microRNA-29a inhibits cancer cell migration and invasion via targeting HSP47 in cervical squamous cell carcinoma. *International Journal of Oncology***43**, 1855-1863, doi:10.3892/ijo.2013.2145 (2013).
- 31 Zhu, J. *et al.* Chaperone Hsp47 Drives Malignant Growth and Invasion by Modulating an ECM Gene Network. *Cancer Research***75**, 1580-1591, doi:10.1158/0008-5472.Can-14-1027 (2015).
- 32 Lee, C.-H. *et al.* The Prognostic Role of STEAP1 Expression Determined via Immunohistochemistry Staining in Predicting Prognosis of Primary Colorectal Cancer: A Survival Analysis. *International Journal of Molecular Sciences***17**, doi:10.3390/ijms17040592 (2016).
- 33 Rodeberg, D. A., Nuss, R. A., Elsawa, S. F. & Celis, E. Recognition of six-transmembrane epithelial antigen of the prostate-expressing tumor cells by peptide antigen-induced cytotoxic T lymphocytes. *Clinical Cancer Research***11**, 4545-4552, doi:10.1158/1078-0432.Ccr-04-2235 (2005).
- 34 Ullio, C. *et al.* Autophagy of metallothioneins prevents TNF-induced oxidative stress and toxicity in hepatoma cells. *Autophagy***11**, 2184-2198, doi:10.1080/15548627.2015.1106662 (2015).
- 35 Zhu, C. *et al.* IFI30 Is a Novel Immune-Related Target with Predicting Value of Prognosis and Treatment Response in Glioblastoma. *Oncotargets and Therapy***13**, 1129-1143, doi:10.2147/ott.S237162 (2020).
- 36 Riihila, P. *et al.* Complement Factor I Promotes Progression of Cutaneous Squamous Cell Carcinoma. *Journal of Investigative Dermatology***135**, 579-588, doi:10.1038/jid.2014.376 (2015).
- 37 Wu, Z. *et al.* Heat Shock Protein 47 Promotes Glioma Angiogenesis. **26**, 31-42, doi:10.1111/bpa.12256 (2016).
- 38 Kerr, F. K. *et al.* Elucidation of the substrate specificity of the C1s protease of the classical complement pathway. *Journal of Biological Chemistry***280**, 39510-39514, doi:10.1074/jbc.M506131200 (2005).
- 39 Vargova, K. *et al.* MYB transcriptionally regulates the miR-155 host gene in chronic lymphocytic leukemia. *Blood***117**, 3816-3825, doi:10.1182/blood-2010-05-285064 (2011).
- 40 Thiele, J.-A. *et al.* lncRNAs in Non-Malignant Tissue Have Prognostic Value in Colorectal Cancer. *International Journal of Molecular Sciences***19**, doi:10.3390/ijms19092672 (2018).

Tables

Table 1 : 163 DEGs were identified from GSE65626, GSE90604, GSE116520 in the patients with GBM to healthy control.

DEGs	Gene Name
Up-regulated	<i>CLIC1, KDELR2, COL4A1, CKS2, TIMP1, VIM, LAMC1, NCAPG, CD44, FCGBP, LAMA4, PYGL, ANGPT2, PDPN, WEE1, TMEM45A, ETS1, CD93, SERPINH1, P4HA1, TGFB111, CALU, ANXA1, ABCC3, TSPAN6, IGF2BP3, GBP2, TNFRSF1A, GAS2L3, GBE1, CCNA2, TPX2, ARHGAP18, GADD45A, DLGAP5, ID3, EZH2, TNC, STEAP3, NAMPT, SLC43A3, IQGAP2, EMP3, CDH11, IFI30, PHLDA1, PLP2, KIF4A, FNDC3B, COL4A2, ADAMTS9, FSTL1, CD163, VEGFA, PRRX1, NES, LMNB1, PLOD2, ANO6, EMP1, FAM20C, SMC4, TNFRSF19, IGFBP5, ITGA5, GBP1, PTGFRN, CALD1, CDCA7L, CFI, ABCA1, HAS2, HIST1H2BK, FAM129A, MIR21, SPRY1, ZNF217, C1S, PCDHB16, KLHDC8A, CRISPLD1, DCBLD2</i>
Down-regulated	<i>PEX5L, RAB11FIP4, NECAB1, UNC13C, DLG2, OPALIN, MAST3, AK5, CACNG3, PCLO, CAMK2A, GRIN1, SYN2, KIAA0513, SLC17A7, RIMS2, GRM3, PPP1R16B, LGI3, TMEM130, CA11, RAPGEF4, SEC14L5, CREG2, NRG1, MAP7D2, NEFM, GNAO1, SYN1, SYT1, SH3GL3, HHATL, SV2B, KIAA1107, SCN2B, PPP2R2C, CNTNAP2, ANKS1B, MAP7, GABRA5, CNTNAP4, MAL, MOBPRUNDC3A, SLC01A2, PPFIA2, PTPRD, NPTX1, ATP2B2, NTSR2, SNAP25, ZNF536, KLHL32, GABRA2, EPB41L4B, RAPGEF5, ATP1B1, CAMKV, DBC1, FA2H, PLLP, NKAIN2, SNAP91, CLDN10, ENPP2, SNCA, SERPINI1, CACNA2D3, KIF1A, MOG, TMEM144, MAG, KLK6, GNG3, CNTN2, PTGDS, ERMN, CNDP1, TF, HSPA2, RCAN2</i>

* The upregulated genes were listed from the largest to the smallest of fold changes, and downregulated genes were listed from the smallest to largest.

* P-value < 0.05 and |Foldchange(FC)| > 1

Table 2 : 21 DEMs were identified from GSE65626, GSE116520 in the Patients with GBM to Healthy Control.

DEMs	Gene Name
Up-regulated	<i>hsa-miR-21-5p, hsa-miR-106b-5p, hsa-miR-210-3p, hsa-miR-18b-5p, hsa-miR-21-3p, hsa-miR-10b-5p, hsa-miR-424-3p, hsa-miR-23a-3p, hsa-miR-195-5p, hsa-miR-371b-5p, hsa-miR-27a-3p, hsa-miR-8063, hsa-miR-5001-5p, hsa-miR-195-3p, hsa-miR-130a-3p, hsa-miR-214-3p, hsa-miR-24-2-5p, hsa-miR-6068, hsa-miR-629-5p, hsa-miR-106b-3p</i>
Down-regulated	<i>hsa-miR-138-2-3p, hsa-miR-874-3p, hsa-miR-874-5p, hsa-miR-139-3p, hsa-miR-184, hsa-miR-338-5p, hsa-miR-330-5p, hsa-miR-770-5p, hsa-miR-323a-3p, hsa-miR-29c-3p, hsa-miR-487b-3p, hsa-miR-6743-5p, hsa-miR-3200-3p, hsa-miR-139, hsa-miR-383-5p, hsa-miR-758-5p, hsa-miR-128-3p, hsa-miR-433-3p, hsa-miR-769-5p, hsa-miR-139-5p, hsa-miR-129-5p, hsa-miR-330-3p, hsa-miR-1250-5p, hsa-miR-338-3p, hsa-miR-770, hsa-miR-29b-3p, hsa-miR-138-5p, hsa-miR-485-5p, hsa-miR-769-3p</i>

* P-value < 0.05 and |Foldchange(FC)| > 1

Table 3 : The miRCODE, miRTarbase, and TargetScan database revealed interactions ceRNA network.

miRNA	mRNA	lncRNA
<i>hsa-miR-29b-3p</i>	<i>SERPINH1</i>	<i>H19 C2orf48 FAM87B C22orf34 HCP5 POLR2J4 LINC00475 UBAC2-AS1 TPRG1-AS1 GAS5 LINC00461 SNHG10 MIR210HG PVT1</i>
<i>has-miR-29c-3p</i>	<i>SERPINH1</i>	<i>H19 C2orf48 FAM87B C22orf34 HCP5 POLR2J4 LINC00475 UBAC2-AS1 TPRG1-AS1 GAS5 LINC00461 SNHG10 MIR210HG PVT1</i>
<i>hsa-miR-139-5p</i>	<i>DCBLD2</i>	<i>LINC00324 HCP5 LINC00152 GAS5 SNHG3 LINC00461 PVT1</i>
<i>hsa-miR-129-5p</i>	<i>C1S</i>	<i>LINC00324 C22orf34 SNHG12 LINC00466 ZNF503-AS1 HCG15 HOTAIR C9orf147 DLEU2 HOTAIRM1 MIR155HG SNHG3 WNT5A-AS1 CRNDE MIR210HG HAS2-AS1 PCAT1 SNHG1</i>

Table 4 : Four lncRNA-miRNA-mRNA networks.

lncRNA	miRNA	mRNA
<i>H19</i>	<i>has-miR-29b-3p</i>	<i>SERPINH1</i>
<i>DLEU2</i>	<i>hsa-miR-29c-3p</i>	<i>SERPINH1</i>
<i>LINC00152</i> <i>LINC00461</i>	<i>has-miR-139-5p</i>	<i>DCBLD2</i>
<i>MIR155HG</i> <i>HOTAIRM1</i> <i>H19</i>	<i>hsa-miR-129-5p</i>	<i>C1S</i>

Figures

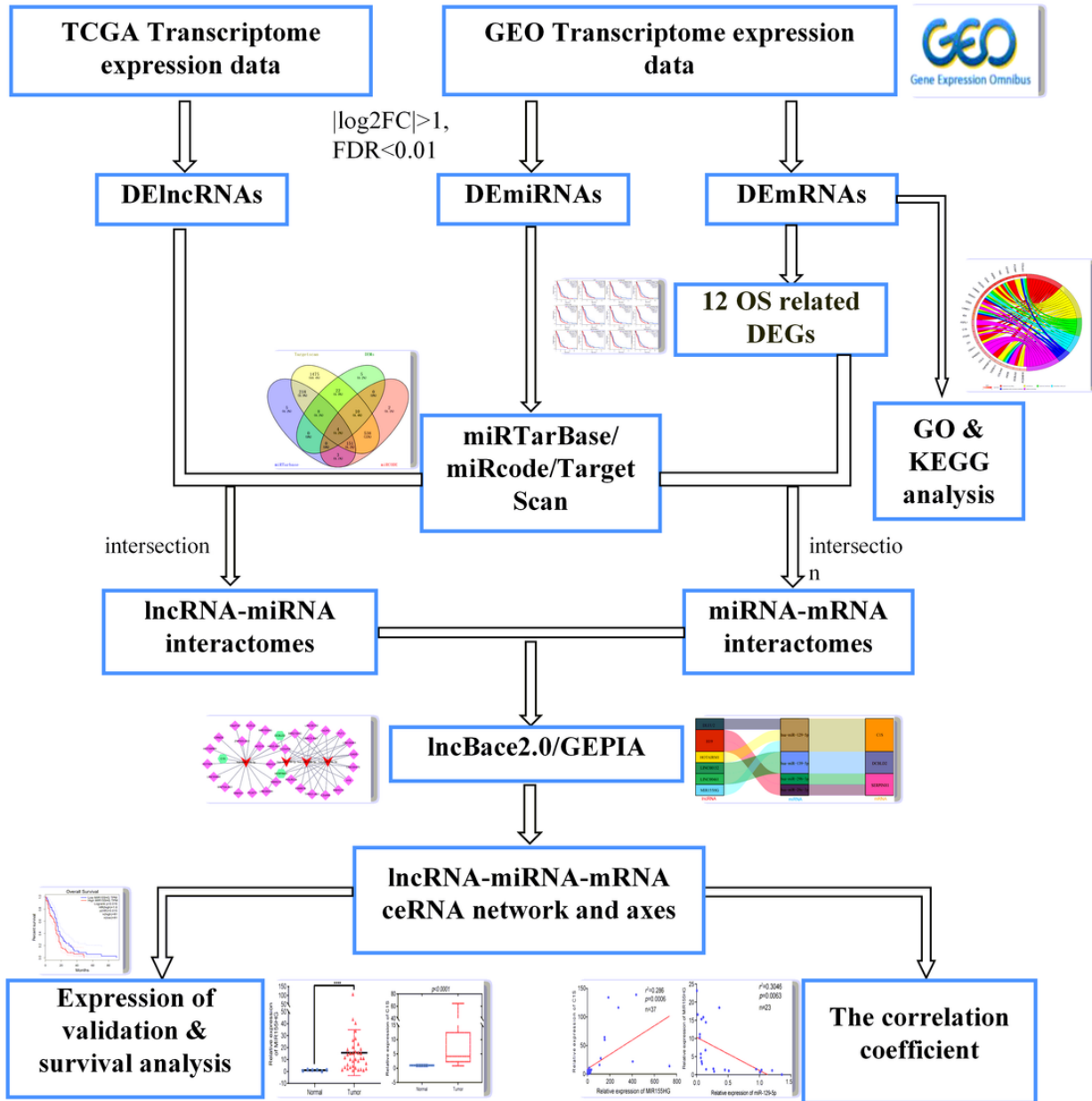


Figure 1

Flow chart of ceRNA network and control axis construction in glioblastoma.

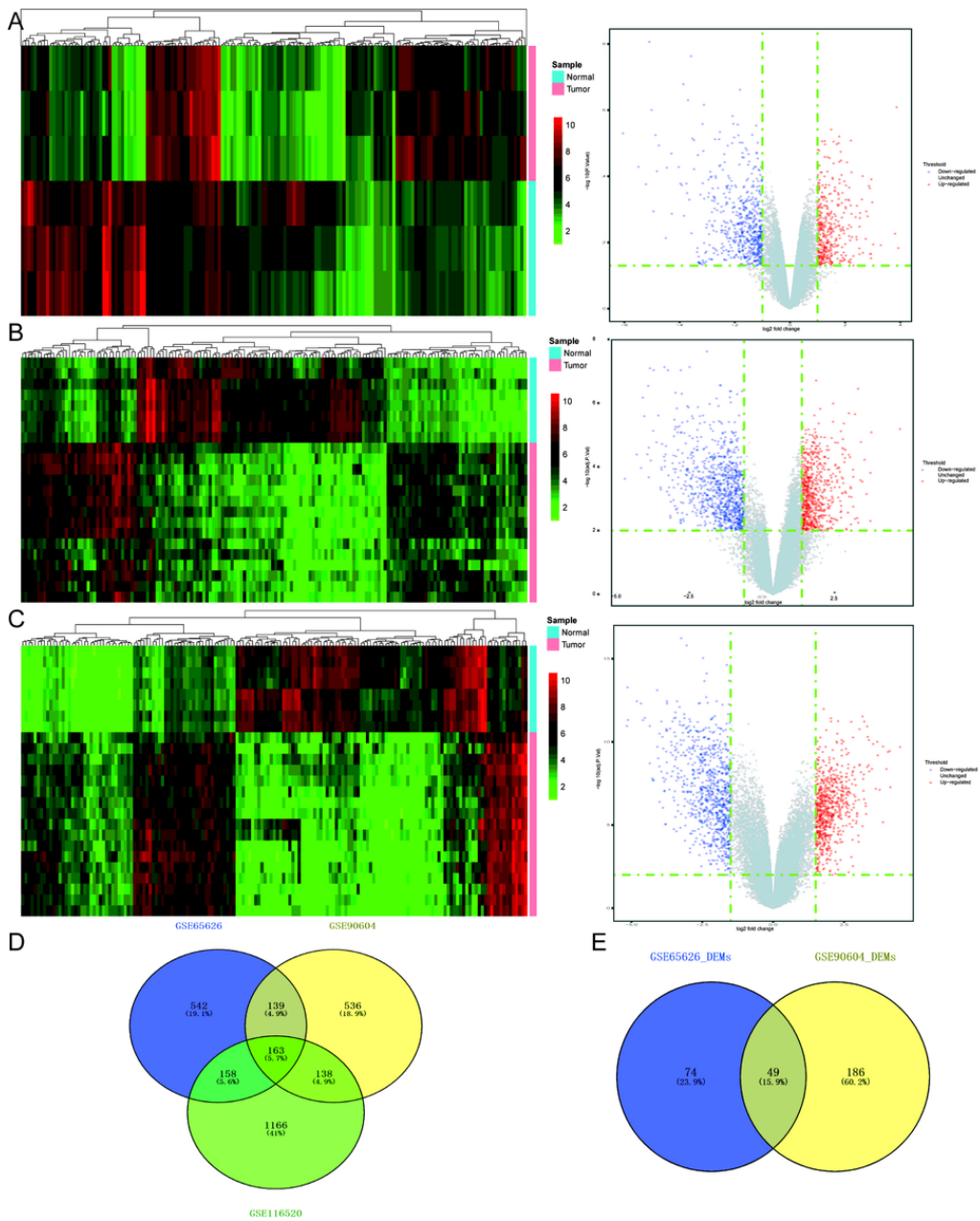


Figure 2

Expression profiles of DEGs and DEMs. (a) Volcano map of DEG expression levels in the GSE65626 dataset. (b) Volcano map of DEG expression levels in the GSE116520 dataset. (c) Heat map of DEGs in the GSE10429 dataset. (d) Heat map of DEGs in the GSE116520 dataset. (e) Venn diagram showing DEGs in the four datasets. (f) Venn diagram showing DEMs in the two microRNA datasets. The red nodes represent upregulated DEGs with FDR-adjusted $p < 0.01$ and $\log_2\text{FC} > 1$ or > 1.5 ; the green nodes represent downregulated DEGs with $p < 0.05$ and $\log_2\text{FC} < -1.0$ or < -1.5 . DEGs: Differentially expressed genes. DEMs: Differentially expressed microRNAs.

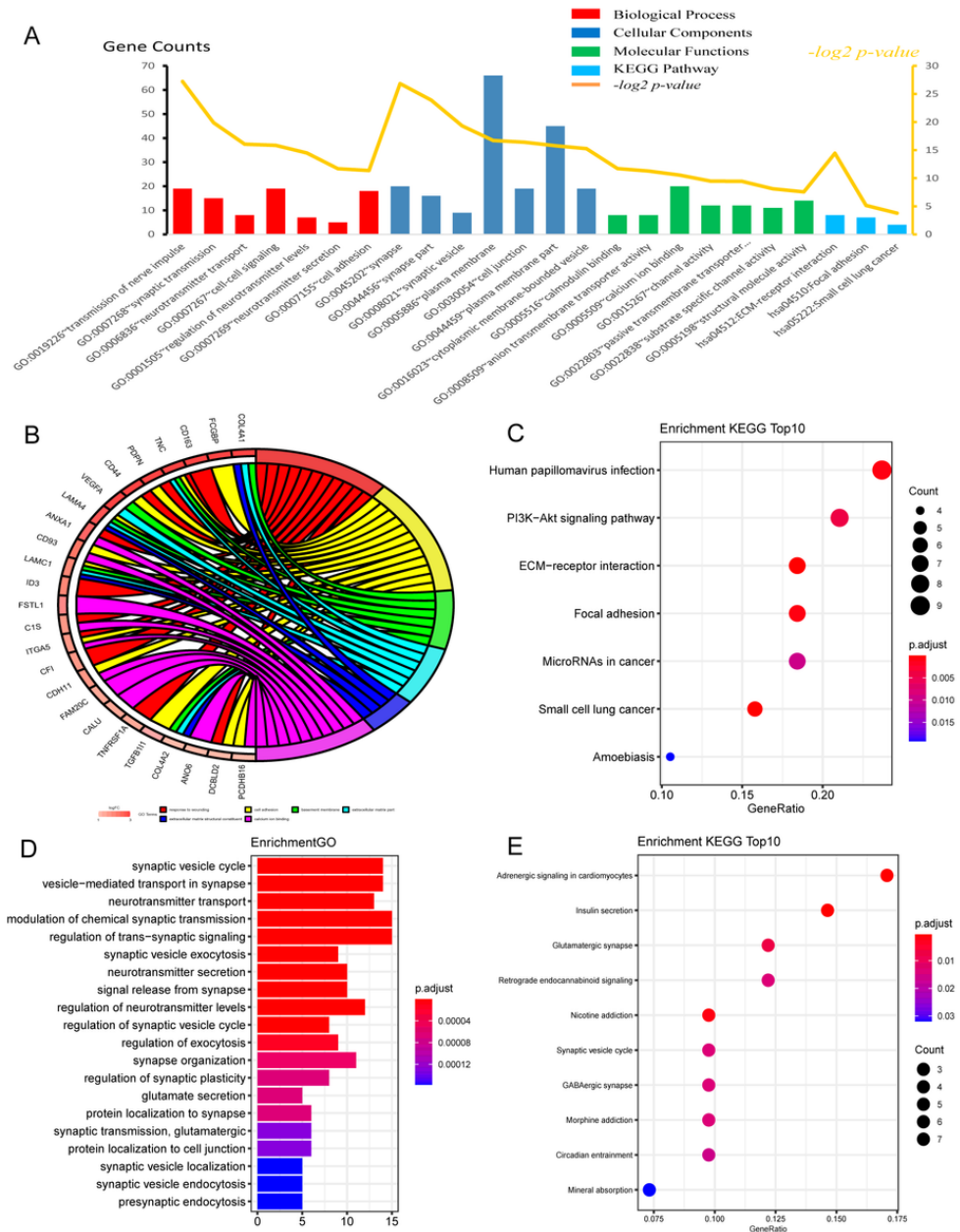
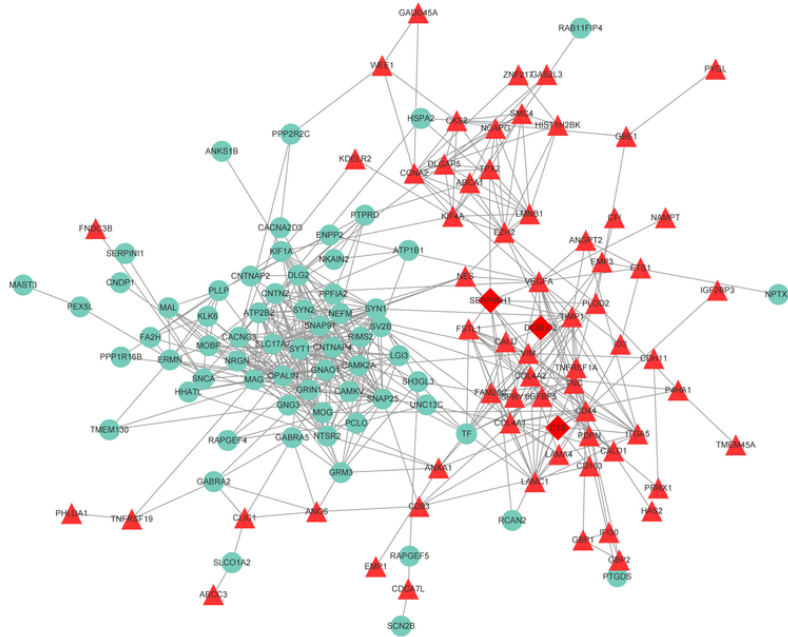


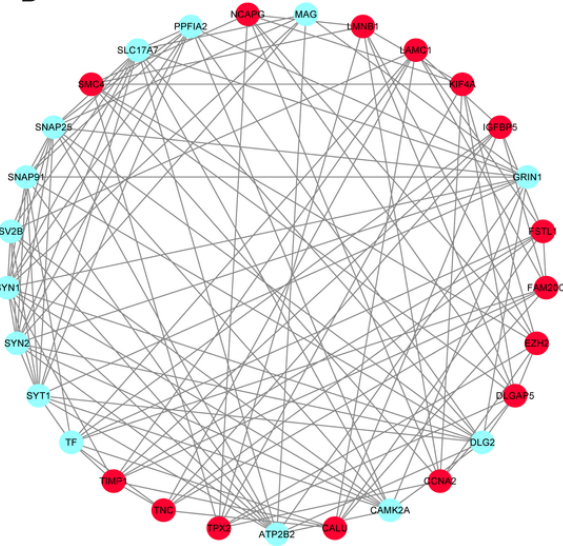
Figure 3

Gene Ontology and Kyoto Encyclopedia of Genes and Genomes enrichment analysis of DEGs. GO enrichment analysis of DEGs. (A) DEGs were classified as BP, CC, or MF. (B-C) Ranking of significantly enriched GO terms for upregulated DEGs. (D-E) Ranking of significantly enriched GO terms for downregulated DEGs. GO: gene ontology, BP: biological process, CC: cellular component, MF: molecular function, DEGs: differentially expressed genes.

A



B



C

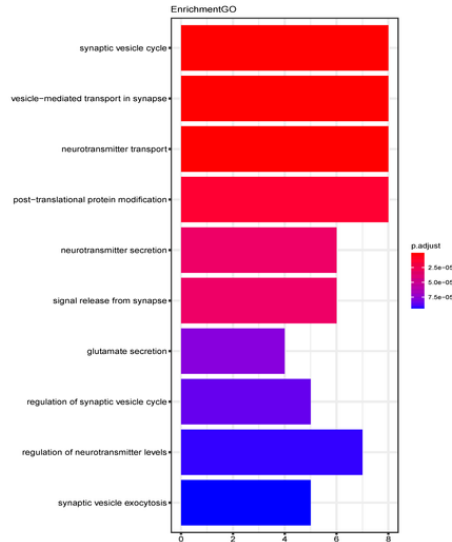


Figure 4

PPI network of DEGs. Node color: red indicates upregulated genes, sky-blue indicates downregulated genes. (A) The PPI network based on the STRING online database contained 132 nodes and 484 edges. (B) The most significant module identified by MCODE (Score = 9.071). (C) GO enrichment analysis of modules. PPI: protein-protein interaction, DEGs: differentially expressed genes, GO: gene ontology.

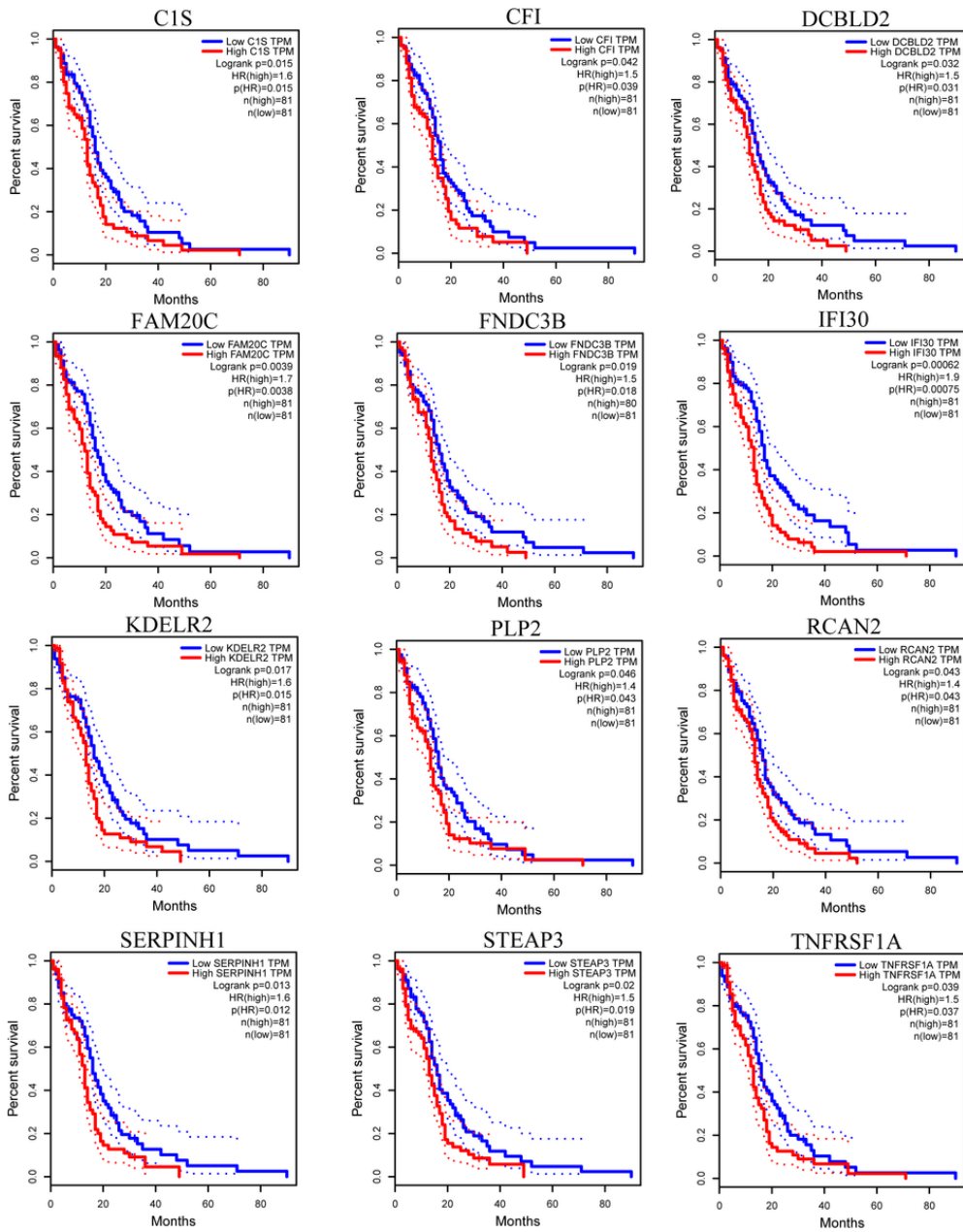


Figure 5

Kaplan-Meier curve of 12 DEGs significantly correlated with overall survival. DEGs: differentially expressed genes.

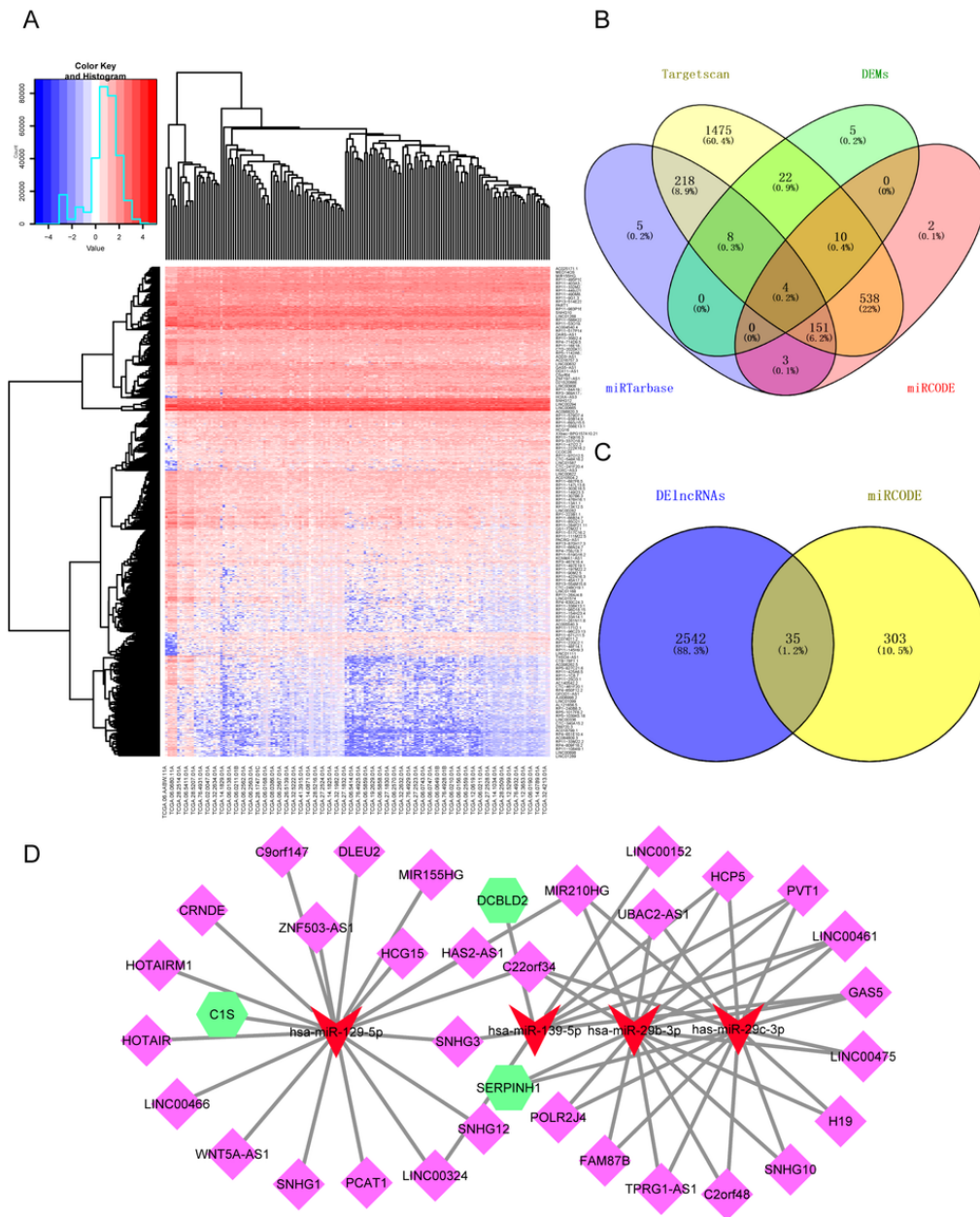


Figure 6

lncRNA-miRNA-mRNA ceRNA network analysis. (A) DElncRNAs from TCGA. DElncRNAs with FDR-adjusted $p < 0.01$ and $\log_{2}FC > 1$ or > 1.5 . (B) Four DEMs conformed to the miRcode, miRTarbase, and TargetScan databases, according to the Venn diagram. (C) Venn diagram showing the 35 intersecting DElncRNAs and 4 DEMs that were predicted using the miRcode website to refine the 1592 identified DElncRNAs. (D) Red represents miRNA upregulation, fluorescent green polygons represent mRNA upregulation, and light purple diamonds represent lncRNA upregulation. DElncRNAs: differentially expressed lncRNAs, TCGA: The Cancer Genome Atlas, DEMs: differentially expressed mRNAs.

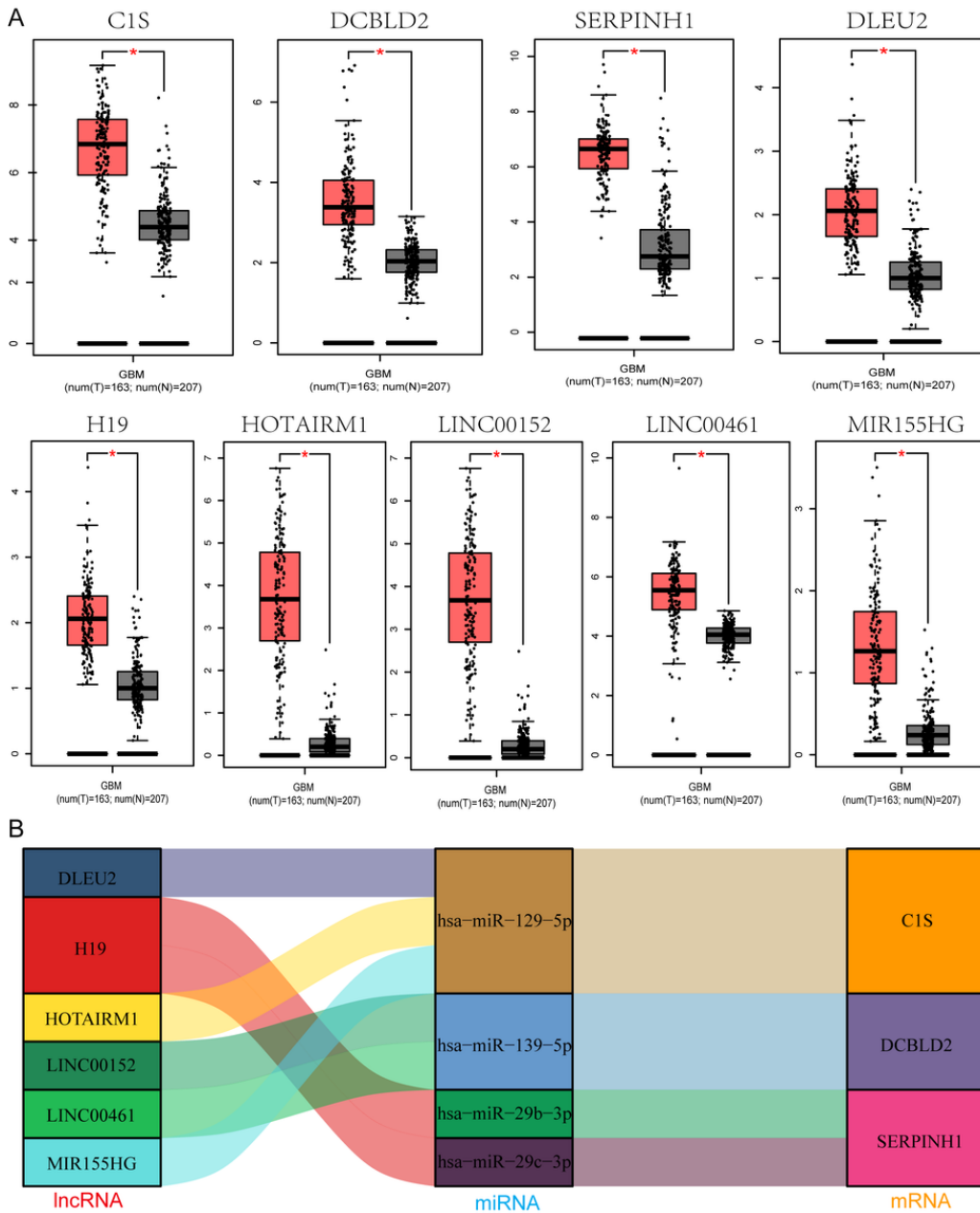


Figure 7

Expression of genes and construction of the GBM lncRNA-miRNA-mRNA network. (A) The expression of seven key genes, including four lncRNAs and three mRNAs, in GBM and normal tissue samples from the GEPIA and lncBace2.0 databases (* $p < 0.05$). (B) Ji mulberry figure revealing four pairs of ceRNA networks: H19/miR-29b-3p/SERPINH1, DLEU2/miR-29c-3p/SERPINH1, LINC00152 LINC00461/miR-139-5p/DCBLD2, and MIR155HG HOTAIRM1 H19/ miR-129-5p/C1S. GBM: glioblastoma, GEPIA: Gene Expression Profiling Interactive Analysis.

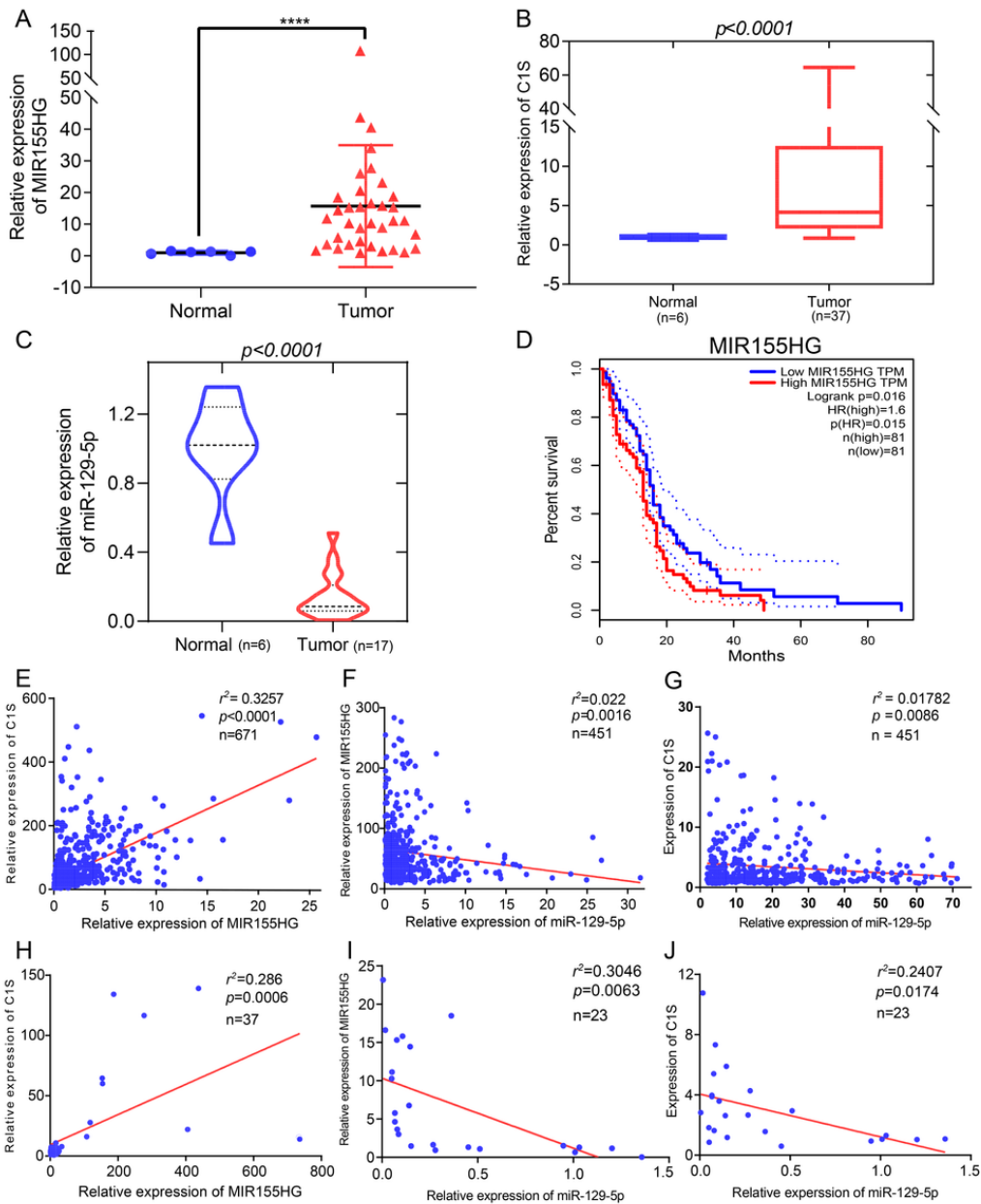


Figure 8

Expression and correlation of the MIR155HG/ miR-129-5p/C1S axis in GBM. (A) The expression of MIR155HG was significantly increased in gliomas compared to that in normal brain tissues, according to the results of qRT-PCR analysis. (B) The expression of miR-129-5p was significantly reduced in gliomas compared to that in normal brain tissues, according to the results of qRT-PCR analysis. (C) The expression of C1S in GBM (n = 37) and normal brain tissue samples collected at our institution. (D) A high level of MIR155HG expression was significantly associated with the overall survival of patients with glioma in the TCGA dataset. (E-G) The correlation between MIR155HG/C1S mRNA, miR-129-5p/MIR155HG, and miR-129-5p/C1S mRNA expression in the TCGA data set was analyzed using the Pearson test. (H-J) The correlation between MIR155HG/C1S mRNA, miR-129-5p/MIR155HG, and miR-129-5p/C1S mRNA expression was analyzed using the Pearson test and qRT-PCR. GBM: glioblastoma, qRT-PCR: real-time quantitative reverse-transcription polymerase chain reaction, TCGA: The Cancer Genome Atlas.